Received: 28 January 2024 | Revised: 26 March 2024 | Accepted: 1 April 2024

DOI: 10.1002/pro.4990

RESEARCH ARTICLE

THE PROTEIN SOCIETY WILEY

Specific features of a scaffolding antibody light chain

Johanna Trommer | **Florian Lesniowski** | **Johannes Buchner** | **Hristo L. Svilenov**

Center of Functional Protein Assemblies (CPA) and School of Natural Sciences, Department of Biosciences, Technical University of Munich, Garching, Germany

Correspondence
Hristo L. Svilenov and Johannes Buchner, Center of Functional Protein Assemblies (CPA) and School of Natural Sciences, Department of Biosciences, Technical University of Munich, Ernst-Otto-Fischer-Straße 8, Garching, 85748, Germany.
Email: hristo.svilenov@ugent.be and johannes.buchner@tum.de

Present address
Hristo L. Svilenov, Faculty of Pharmaceutical Sciences, Ghent University, Ottergemsesteenweg 460, Ghent, 9000, Belgium.

Funding information
Else Kröner-Fresenius-Stiftung, Grant/Award Number: 2020_EKEA.31; Peter und Traudl Engelhorn Stiftung

Abstract

The antigen-binding sites in conventional antibodies are formed by hypervariable complementarity-determining regions (CDRs) from both heavy chains (HCs) and light chains (LCs). A deviation from this paradigm is found in a subset of bovine antibodies that bind antigens via an ultra-long CDR. The HCs bearing ultra-long CDRs pair with a restricted set of highly conserved LCs that convey stability to the antibody. Despite the importance of these LCs, their specific features remained unknown. Here, we show that the conserved bovine LC found in antibodies with ultra-long CDRs exhibits a distinct combination of favorable physicochemical properties such as good secretion from mammalian cells, strong dimerization, high stability, and resistance to aggregation. These physicochemical traits of the LCs arise from a combination of the specific sequences in the germline CDRs and a lambda LC framework. In addition to understanding the molecular architecture of antibodies with ultra-long CDRs, our findings reveal fundamental insights into LC characteristics that can guide the design of antibodies with improved properties.

KEYWORDS

antibodies, antibody light chains, protein stability, ultra-long CDRs

1 | INTRODUCTION

In most mammalian antibodies, the complementarity-determining regions (CDRs) from both the heavy chain (HC) and the light chain (LC) form the antigen-binding site. There are only a few exceptions to this paradigm such as the HC-only antibodies in camelids (Hamers-Casterman et al., 1993) and the antibodies with ultra-long CDR-H3s in cattle (Wang et al., 2013). The latter are a special case because the binding to the antigen is solely via an ultra-long CDR-H3 (Stanfield et al., 2020; Wang et al., 2013). The ultra-long CDR can contain up to 70 residues folded as a characteristic "stalk and knob" structure (Passon et al., 2023; Wang et al., 2013). We have previously dissected the importance of the different structural elements in the ultra-long CDR, showing that the stalk conveys stability allowing for large structural variations in the knob domain (Svilenov et al., 2021).

Each species has a set of germline variable (V), diversity (D), and joining (J) antibody gene segments (de los Rios et al., 2015). Different assembly of these segments via a process called V(D)J recombination followed by somatic hypermutation (SHM) is the basis for antibody diversity (Chi et al., 2020). Pairing between HCs and LCs

Reviewing Editor: Aitziber L. Cortajarena

from different germline segments creates additional variation in antibody repertoires (Jayaram et al., 2012). In cows, there are 12 IGHV, 16 IGHD, and 4 IGHJ functional segments (Deiss et al., 2019; Ma et al., 2016). Interestingly, a specific combination of V, D, and J segments (IGHV1-7, IGHD8-2, IGHJ2-4) is utilized in the HCs of antibodies with ultra-long CDRs (Deiss et al., 2019; Li et al., 2023; Stanfield et al., 2016). The LC germline genes can be assigned to one of two types—lambda (λ) or kappa (κ). Cows almost exclusively employ λ LCs formed by approximately 17 functional V-J combinations of IGLV and IGLJ segments (Liljavirta et al., 2014).

Despite an immense sequence diversity in the knob, the HCs from antibodies with ultra-long CDR-H3s pair almost exclusively with highly conserved LCs from the V30 germline (Saini et al., 2003). V30 LCs, such as BOV LC (Dong et al., 2019) and NC-Cow1 LC (Sok et al., 2017), are abundantly expressed in cattle and likely play an important role in ensuring the stability of antibodies with ultra-long CDRs (Liljavirta et al., 2014).

Interestingly, the LCs from antibodies with ultra-long CDRs do not contribute to the antigen-binding site (Adams et al., 2023; Hawkins et al., 2022; Macpherson et al., 2020; Macpherson et al., 2021; Stanfield et al., 2020). Therefore, it appears that there is no evolutionary pressure on these LCs towards antigen binding. As a result, there is likely no or only a minimal requirement that the LC achieves a delicate balance between optimal antigen binding properties and sufficient intrinsic stability (Rabia et al., 2018). Consequently, it seems that the conserved V30 LCs present a case where evolution selected variable antibody domains mainly for their structural and stabilizing role. However, despite the growing number of studies on the ultra-long CDRs (Passon et al., 2023), little is known about the features of the V30 LCs. Their analysis could reveal new insights into structural principles of natural antibodies.

Here we report that the bovine LC found in antibodies with ultra-long CDRs exhibits distinct biophysical features such as good secretion from mammalian cells, pronounced dimerization, high stability, and resistance to aggregation. We track the origin of these features to a combination of a λ LC and highly conserved CDRs with a characteristic amino acid composition that could inform the design of antibodies with improved physiochemical properties.

2 | RESULTS

2.1 | Conserved bovine LC exhibits distinct biophysical traits

To test whether there are differences in structure and stability between LCs from canonical antibodies and antibodies with ultra-long CDRs from cows, we selected four model bovine LCs: BOV LC and NC-Cow1 LC are from antibodies bearing ultra-long CDRs, while B4 LC and B13 LC are from antibodies with conventional CDRs (Dong et al., 2019; Ren et al., 2019; Sok et al., 2017). Sequence alignment indicates high homology between the four LCs (Figure 1a). NC-Cow1 and BOV differ only by 10 residues in the V_L (Figure 1a). When we expressed these LCs in mammalian cells, we found that all except for B4 are secreted well (Figure 1b). Upon purification of the LCs from the cell supernatants, we obtained monomers and homodimers with interchain disulfide bonds (covalent dimers) from NC-Cow1 LC and BOV LC as evident from sodium dodecyl sulfate polyacrylamide gel electrophoresis (SDS-PAGE) (Figure S1). Only monomers could be purified for B13 LC. To investigate the oligomeric state of the LCs under native conditions, we used size exclusion chromatography coupled with multi-angle light scattering (SEC-MALS). The covalent dimers elute as narrow peaks with molecular masses around 45 kDa (Figure 1c). Interestingly, the LCs that run as monomers in nonreducing SDS-PAGE exhibit distinct behavior under native conditions in SEC-MALS (Figure 1d). BOV LC elutes as one peak with a mass ~40 kDa, which indicates strong non-covalent homo-dimerization. NC-Cow1 LC elutes as a mixture of monomers and dimers with apparent masses spanning 20–40 kDa. The major fraction of B13 LC elutes as a monomer with a mass of about 22 kDa and a small dimer peak. Overall, SEC-MALS indicates that BOV LC monomers exhibit stronger dimerization propensities under native conditions compared to the NC-Cow1 counterpart. B13 LC has a weaker dimerization tendency compared to the other two LCs.

To compare their structures and thermal stabilities, we assayed the LCs by far-UV circular dichroism (FUV-CD) spectroscopy. The covalent dimers NC-Cow1 and BOV LCs have superimposable FUV-CD spectra (Figure 1e). However, the dimeric NC-Cow1 LC has a T_M of 50.2, while the BOV counterpart has a T_M of 64.2 °C (Figure 1f; Table 1). Remarkably, FUV-CD suggests that the structures of the dimeric bovine LCs are preserved after incubation at 95 °C and subsequent cooling to room temperature (Figure S2). SEC-MALS analysis revealed that the covalent dimer of BOV LC is resistant to aggregation even after heating to temperatures above the T_M (Figure 1g). In contrast to the covalent dimers, the secondary structure of the monomeric LCs is different as suggested by FUV-CD spectra (Figure 1h). The LC monomers of NC-of Cow1, BOV, and B13 have T_Ms of 51.0 °C, 59.7 °C, and 58.5 °C, respectively (Table 1). Interestingly, the covalent dimer of BOV LC is almost 5 °C more stable than the monomer, while the monomer and dimer of NC-Cow1 LC have approximately the same stability as

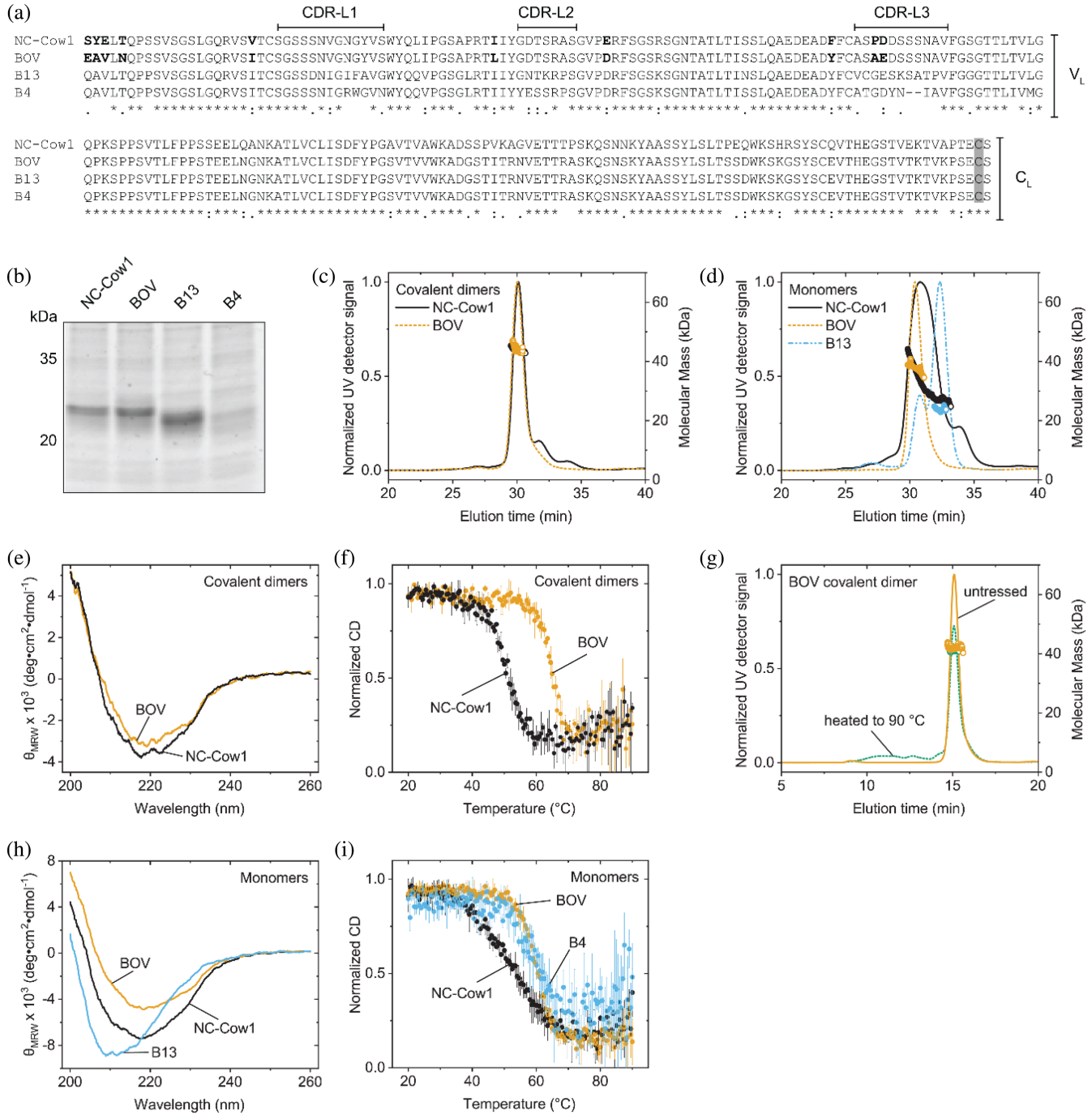

FIGURE 1 Features of natural bovine LCs from antibodies with conventional or ultra-long CDRs. (a) Sequence alignment of the V_L and C_L domains of the four bovine LCs. The residues in bold indicate differences between the two LCs found in antibodies with ultra-long CDRs. The cysteine residue marked by a gray background can form an intermolecular disulfide bond in LC homodimers. In antibodies, these LC cysteines form an intermolecular disulfide bond with the C-terminal cysteine in the C_H1 domain. (b) Reducing SDS-PAGE on Expi293 supernatants transfected for secretion of LCs. (c) SEC-MALS of disulfide-linked LC dimers. (d) SEC-MALS of monomeric LCs. (e) FUV-CD spectra of disulfide-linked LC dimers. (f) Thermal unfolding of disulfide-linked LC dimers tracked with FUV-CD by the ellipticity change at 202 nm. (g) SEC-MALS analysis of BOV LC dimer before and after incubation for 5 min at 90 °C (elution flow rate of 1 mL/min was used in this experiment). (h) FUV-CD spectra of LC monomers. (i) Thermal unfolding of LC monomers tracked with FUV-CD by the ellipticity change at 202 nm. CDRs, complementarity-determining regions; FUV-CD, far-UV circular dichroism; LC, light chain; SEC-MALS, size exclusion chromatography coupled to multi-angle light scattering; SDS-PAGE, sodium dodecyl sulfate polyacrylamide gel electrophoresis.

TABLE 1 Summary of LC properties.

LC variant	Secretion		T_M (°C)	
	Monomer	Covalent dimer	Monomer	Covalent dimer
Wildtype				
NC-Cow1	Good	Good	51.0 ± 0.1	50.2 ± 0.1
BOV	Good	Good	59.7 ± 0.1	64.2 ± 0.2
B4	Poor	Poor	n.d.	n.d.
B13	Good	Poor	58.5 ± 0.8	n.d.
PGT145	Poor	Poor	n.d.	n.d.
109L	Good	Good	51.1 ± 1.6	
C_L mutants				
BOV_{VL}-$PGT145_{CL}$	Good	Poor	54.2 ± 0.7	n.d.
BOV_{VL}-$109L_{CL}$	Good	Good	60.5 ± 0.1	66.0 ± 0.7
$PGT145_{VL}$-BOV_{CL}	Poor	Poor	n.d.	n.d.
$109L_{VL}$-BOV_{CL}	Good	Poor	45.9 ± 0.5	n.d.
CDR mutants				
BOV-$PGT145_{CDRs}$	Good	Poor	51.5 ± 0.5	n.d.
BOV-$109L_{CDRs}$	Poor	Good	n.d.	54.1 ± 0.2
PGT145-BOV_{CDRs}	Good	Poor	54.2 ± 0.4	n.d.
109L-BOV_{CDRs}	Good	Good	52.3 ± 0.5	54.1 ± 0.1

Note: The "good" and "bad" annotation for the secretion is based on whether a distinct band could be observed in SDS-PAGE from the supernatants of transfected cells and whether the mass of the purified LC from the supernatant was verified.
Abbreviations: LC, light chain; SDS-PAGE, sodium dodecyl sulfate polyacrylamide gel electrophoresis.

indicated by the T_M. Overall, the analysis of the LCs reveals remarkable features of the natural BOV LC such as strong homo-dimerization, high T_M, and resistance to aggregation at temperatures above the T_M and reversible thermal unfolding.

2.2 | Importance of the bovine C_L domain

To test to what extent the bovine C_L domain contributes to the features of BOV LC, we created LC variants in which we exchanged the C_L in BOV LC (λ) with the C_L from a human λ or κ antibody—109L LC (λ) and PGT145 LC (κ), respectively (Garces et al., 2015; Lee et al., 2017) (Figure 2a). We selected these human LCs for two reasons. First, we have previously produced and characterized the LCs with their natural HC counterparts as heterodimers (Svilenov et al., 2021). Second, there are different sequence identities between the two human LCs and BOV LC: ~63% and ~40% for 109L LC and PGT145 LC, respectively. We obtained monomers and disulfide-linked dimers for BOV_{VL}-$109L_{CL}$, while BOV_{VL}-PGT_{CL} yielded only monomers (Figure S1). Strikingly, BOV_{VL}-$109L_{CL}$ monomer shows similar non-covalent homodimerization in SEC-MALS compared to wildtype BOV LC (Figure 2b). In contrast, BOV_{VL}-PGT_{CL} is monomeric under native conditions. The disulfide-linked dimer of BOV_{VL}-$109L_{CL}$ and the wildtype BOV counterpart have almost identical chromatograms (Figure 2e). Consistent with the SEC-MALS results, FUV-CD spectroscopy indicates that the structure of the monomeric BOV_{VL}-PGT_{CL} is different compared to monomeric BOV LC while the spectra of BOV_{VL}-$109L_{CL}$ and BOV LC monomers are nearly identical (Figure 2c). The FUV-CD spectrum of disulfide-linked dimers of BOV LC is superimposable with the spectrum of dimeric BOV_{VL}-$109L_{CL}$ (Figure 2f). Thermal stability analysis revealed equivalent stability for BOV LC and BOV_{VL}-$109L_{CL}$ (Figure 2d,g; Table 1). In contrast, the monomeric BOV_{VL}-PGT_{CL} chimera exhibits an about 6 °C lower T_M compared to monomeric BOV LC (Figure 2d; Table 1). The structure of monomeric and dimeric BOV_{VL}-$109L_{CL}$ is slightly affected after short heat stress (5 min, 95 °C), while the structure of BOV_{VL}-PGT_{CL} is severely perturbed under the same conditions (Figure S3). In addition, we also wondered whether the C_L domain is important for the secretion of the LCs and attempted to produce the isolated V_L in mammalian cells, but the secretion levels were very low (Figure S4). Taken together, these results show an important role of the C_L domain for the secretion, dimerization, and stability of BOV LC. Remarkably, exchanging the

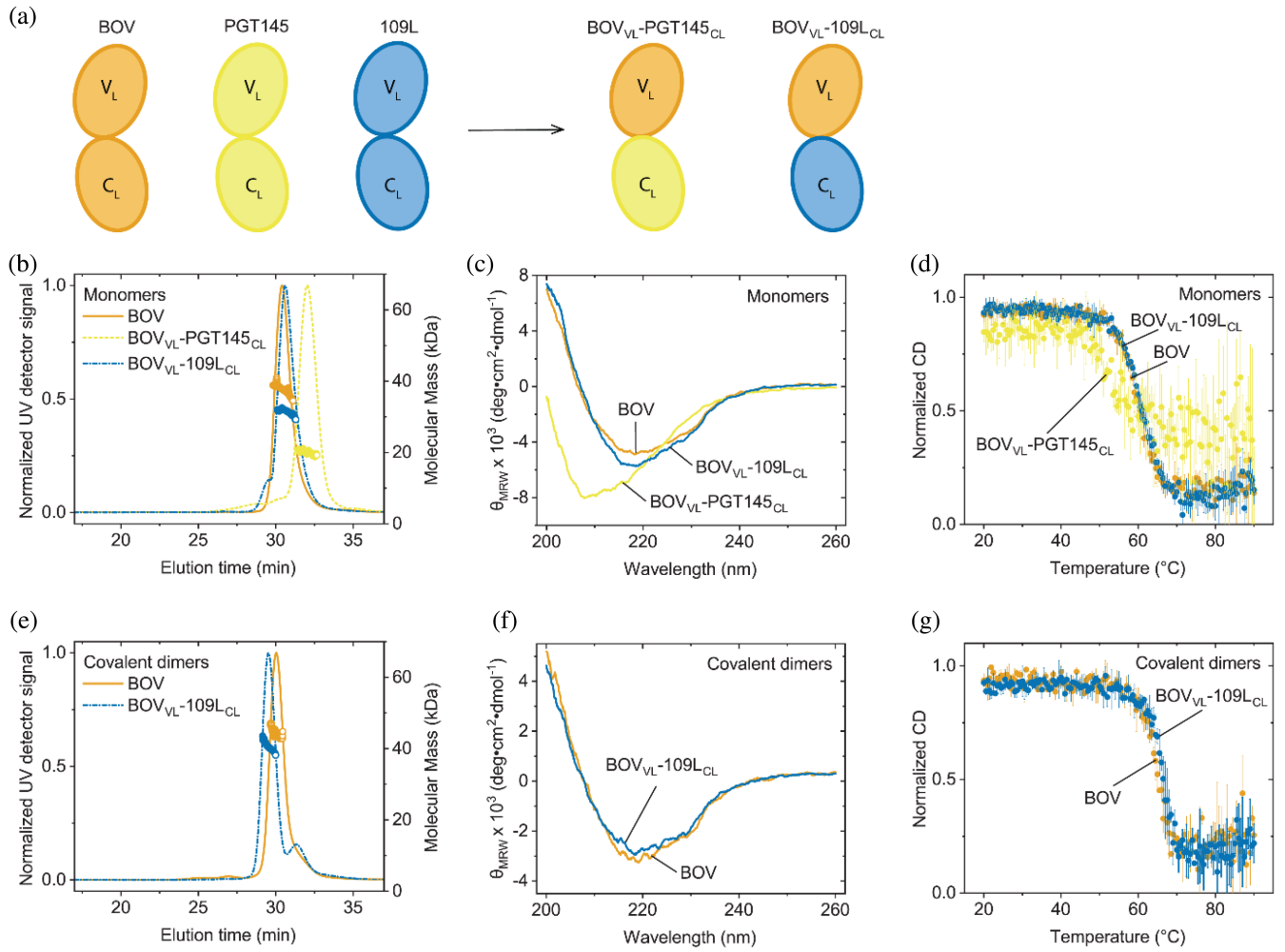

FIGURE 2 The C_L domain is important for the biophysical features of BOV LC. (a) Three wildtype light chains, BOV (λ, bovine), PGT145 (κ, human) and 109L (λ, human), were used to create LC chimeras with a bovine V_L and a human C_L domain. (b) SEC-MALS of LC monomers. (c) FUV-CD spectra of LC monomers. (d) Thermal unfolding of LC monomers monitored by the ellipticity change at 202 nm. (e) SEC-MALS of disulfide-linked LC dimers. (f) FUV-CD spectra of disulfide-linked LC dimers. (g) Thermal unfolding of disulfide-linked LC dimers monitored by the ellipticity change at 202 nm. FUV-CD, far-UV circular dichroism; LC, light chain; SEC-MALS, size exclusion chromatography coupled to multi-angle light scattering.

bovine λ C_L with a human λ C_L had minimal impact on the biophysical features of BOV LC. However, the exchange to a κ C_L was not well tolerated.

2.3 | Importance of the conserved bovine CDRs

The LCs in antibodies with ultra-long CDRs undergo minimal or no affinity maturation and their CDRs play only a structural role (Dong et al., 2019; Stanfield et al., 2018; Wang et al., 2013). We therefore wondered whether the conserved CDRs contribute to the dimerization and stability of BOV LC. To this end, we produced BOV LC mutants in which we exchanged all three CDRs with the CDRs from the human 109L or PGT145 LCs, respectively (Figure 3a). The two chimeric LCs were secreted well by mammalian cells, but only monomers could be purified for BOV-PGT145$_{CDRs}$, while purification of BOV-109L$_{CDRs}$ yielded disulfide-linked dimers (Figure S1). In SEC-MALS analyses, monomeric BOV-PGT145$_{CDRs}$ shows weaker homodimerization tendency ($M_m \sim 21$ kDa) under native conditions compared to the monomeric BOV LC ($M_m \sim 39.8$ kDa) (Figure 3b). The elution of the covalent homodimers of BOV is similar to that of the BOV-109L$_{CDRs}$ (Figure 3e). Interestingly, BOV-109L$_{CDRs}$ exhibits differences in the FUV-CD spectrum compared to BOV LC and BOV-PGT145$_{CDRs}$ (Figure 3c,f). For both chimeric LCs, the thermal stability was reduced by ~8–10 °C compared to the natural BOV LC counterparts (Figure 3d,g; Table 1). In addition, both exhibit substantial nonreversible structural changes upon

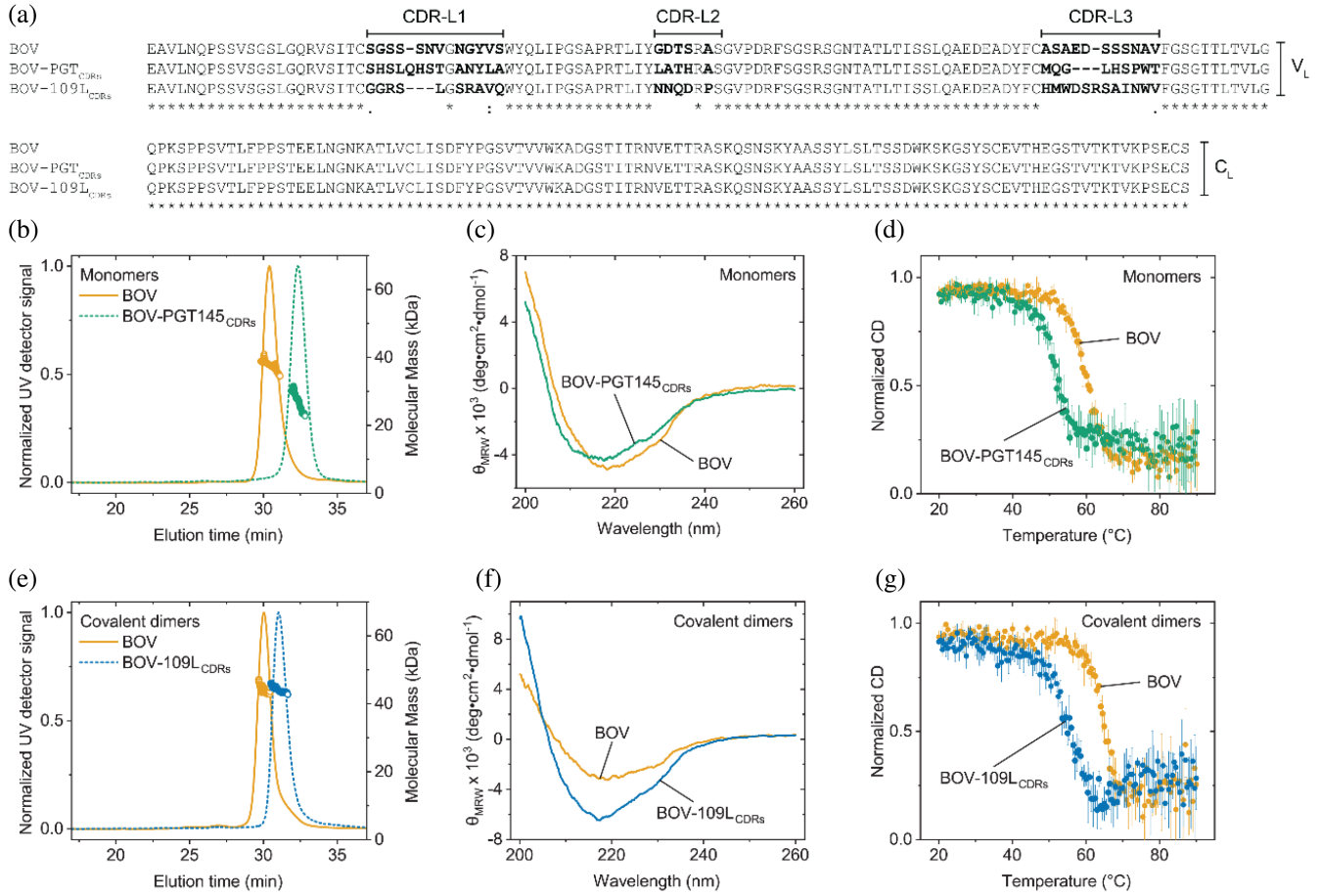

FIGURE 3 The CDRs are essential for BOV LC dimerization, structure, and stability. (a) Sequence alignment of natural BOV LC and two chimeric LCs with human CDRs on a BOV LC scaffold. (b) SEC-MALS of LC monomers. (c) FUV-CD spectra of LC monomers. (d) Thermal unfolding of LC monomers tracked with FUV-CD by the ellipticity change at 202 nm. (e) SEC-MALS of disulfide-linked LC dimers. (f) FUV-CD spectra of disulfide-linked LC dimers. (g) Thermal unfolding of disulfide-linked LC dimers tracked by the ellipticity change at 202 nm. CDRs, complementarity-determining regions; FUV-CD, far-UV circular dichroism; LC, light chain; SEC-MALS, size exclusion chromatography coupled to multi-angle light scattering.

exposure to high temperatures (5 min, 95 °C) (Figure S3). Overall, these findings reveal an important role of the conserved bovine CDRs for the biophysical features of the BOV LC.

2.4 | Transferring bovine LC elements into human LCs

After learning that both the C_L and the CDRs contribute to the extraordinary features of BOV LC, we were interested in whether bovine LC building blocks can convey improved biophysical properties in human LCs. We therefore created variants of the human LCs PGT145 and 109L where we combined the human V_Ls with the C_L from BOV LC (PGT145$_{VL}$-BOV$_{CL}$ and 109L$_{VL}$-BOV$_{CL}$) or replaced the human CDRs with the BOV LC CDRs (PGT145-BOV$_{CDRs}$ and 109L-BOV$_{CDRs}$). Remarkably, the bovine CDRs, but not the C_L, restore the secretion of PGT145 LC (Figure 4a). In contrast, the bovine sequences have little impact on the secretion of 109L, which is already well-secreted as a wildtype (Figure 4b). Next, we purified monomeric 109L-BOV$_{CDRs}$ and 109L$_{VL}$-BOV$_{CL}$, as well as covalent dimers of 109L-BOV$_{CDRs}$. Despite optimizations, we could obtain only a mixture of monomers and covalent dimers of wildtype 109L (Figure S1). Wildtype 109L elutes as multiple peaks in SEC-MALS (Figure 4c). 109L$_{VL}$-BOV$_{CL}$ monomer elutes as a broad peak corresponding to a mixture of monomers and non-covalent homodimers (Figure 4d). In contrast, 109L variants with CDRs from BOV LC gave narrow symmetric peaks with the expected mass for a monomer (Figure 4d) and a covalent dimer (Figure 4e). Wildtype 109L has a T_M of 51.1 °C, while the 109L$_{VL}$-BOV$_{CL}$ has a T_M of 45.9 °C (Figure 4f,g; Table 1). Monomer and covalent dimer of 109L-BOV$_{CDRs}$ have T_Ms of 52.3 °C and 54.1 °C,

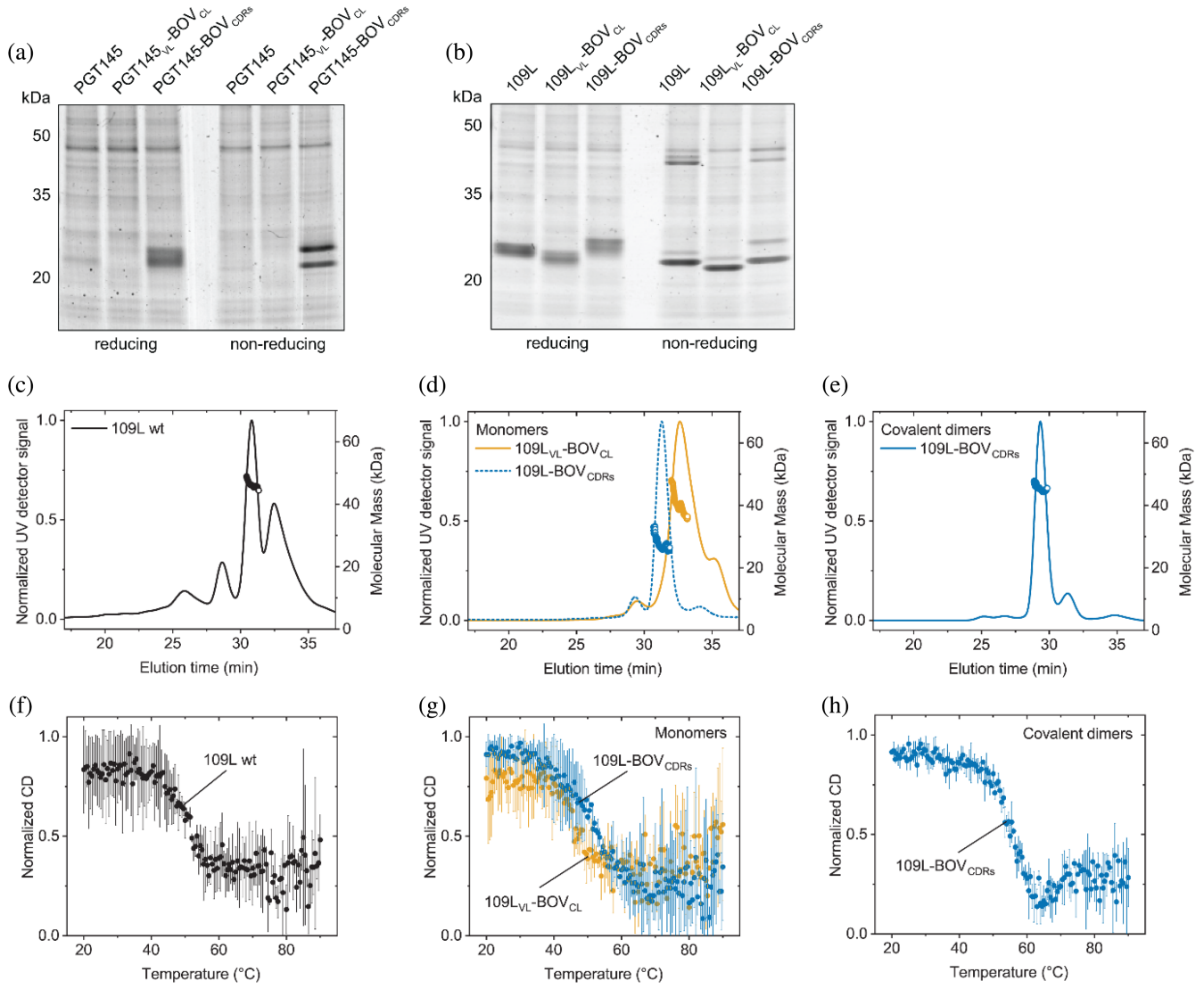

FIGURE 4 Impact of BOV LC C_L or CDRs on the properties of human LCs. (a) SDS-PAGE on Expi293 supernatants transfected for secretion of PGT145 LC variants. (b) SDS-PAGE on Expi293 supernatants transfected for secretion of 109L LC variants. (c) SEC-MALS of wildtype 109L. (d) SEC-MALS of monomeric 109L variants. (e) SEC-MALS of covalent dimer of 109L-BOV_{CDRs}. (f–h) Thermal unfolding of LC variants tracked with FUV-CD by the ellipticity change at 202 nm. FUV-CD, far-UV circular dichroism; LC, light chain; SDS-PAGE, sodium dodecyl sulfate polyacrylamide gel electrophoresis; SEC-MALS, size exclusion chromatography coupled to multi-angle light scattering.

respectively (Figure 4g,h; Table 1). Therefore, the bovine CDRs from BOV LC can convey improved secretion, reduce heterogeneity, and increase the thermal stability of human LCs.

2.5 | Effect of bovine, human, and chimeric LCs on fab secretion

Finally, we asked how the LCs affect the assembly and secretion of Fab fragments (Svilenov et al., 2021). To address this question, cells were transfected with plasmids for the LCs or HCs (Fd segments), or co-transfected with a combination of the LC and Fd plasmids. The Fd segments were not secreted because C_H1 domains are retained in the endoplasmic reticulum in the absence of C_L domains (Figure S5) (Feige et al., 2009). In contrast, the LCs of BOV-7 and NC-Cow1 were secreted as monomers and dimers (Figure S5a). Upon co-transfection with different LC/Fd plasmid ratios, the bovine Fabs were secreted well at a 1:1 LC/Fd ratio. Higher LC/Fd ratios of 3:1 and 4:1 did not lead to a further improvement in Fab secretion but caused secretion of LC monomers and dimers (Figure S5a). In contrast, the secretion of the human Fab 32H109L was gradually improved by using higher LC/Fd ratios and no free human LC (109L) was detected (Figure S5b). When the human Fd (32H) was co-transfected with the chimeric 109L-BOV_{CDRs}, the

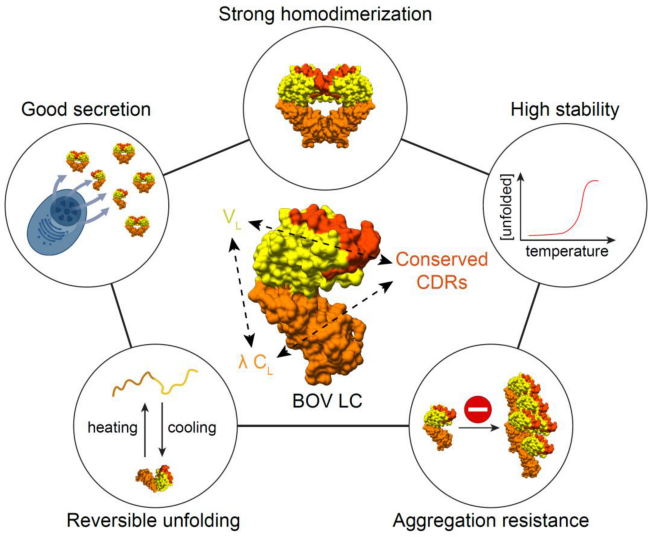

FIGURE 5 Summary of distinct traits in the conserved BOV LC. LC, light chain.

secretion of the Fab was improved and free 109L-BOV_{CDRs} LC was detected at higher LC/Fd ratios as well (Figure S5b). Therefore, a chimeric LC carrying structural elements from BOV LC can facilitate the assembly and secretion of a Fab fragment.

3 | DISCUSSION

We found that an invariant BOV LC has remarkable biophysical traits that emerge from a combination of a bovine λ C_L and the V_L with CDRs encoded by the V30 germline (Figure 5). BOV LC is almost identical to the V30 germline sequence with only two differences at Kabat positions one (E instead of Q) and five (N instead of T) (Stanfield et al., 2020). In contrast, NC-Cow1 LC has nine mutations compared to the germline (Stanfield et al., 2020). Consequently, NC-Cow1 LC exhibits greatly reduced stability compared to BOV LC (Figure 1). This reveals that the bovine V30 germline encodes exceptional biophysical traits that are maintained in highly conserved LCs such as BOV LC, likely due to a lack of evolutionary pressure for CDR affinity maturation toward antigen binding via the LC.

The favorable features encoded by V30 were likely essential for the emergence of antibodies with ultra-long CDRs since the HCs of these antibodies assemble almost exclusively with V30 LCs. In addition, the same V30 LC, such as BOV LC, can pair with HCs that bear structurally very diverse ultra-long CDR-H3s (Dong et al., 2019). Other antibodies with paratopes formed entirely by the HC, such as the HC-only antibodies in camelids and the immunoglobulin new antigen receptor in sharks, are devoid of LCs (Greenberg et al., 1995; Hamers-Casterman et al., 1993). Therefore, it is interesting that the bovine antibodies with ultra-long CDRs followed a different evolutionary trajectory that maintained the LC for stability reasons.

Remarkably, replacing the λ C_L in BOV LC with a human λ C_L had little impact on the biophysical traits. In contrast, a human κ C_L severely impacted the homodimerization, structure, and stability of the LC. When we replaced the CDRs of BOV LC with the CDRs from human LCs, we observed negative effects on stability and homodimerization. This points toward a key role of the V_L and CDRs encoded by V30, which, in combination with a λ C_L, convey a combination of favorable biophysical traits (Figure 5).

We wondered what makes BOV LC special and looked at the amino acid usage in the V_L and the CDRs (Figure 1a). Interestingly, BOV V_L contains multiple serine residues (20.7%), only one highly conserved tryptophan and no histidine, lysine, or methionine. The calculated isoelectric point is around 4.4. Noteworthy, acidic isoelectric points were linked to rare properties in antibody domains such as reversible thermal unfolding and high resistance to aggregation at high temperatures (Jespers et al., 2004). In the CDRs of BOV LC, serine is even more abundant (35.5%), there is only one positively charged (R) and three negatively charged residues (2× D, 1× E). Overall, a high serine usage combined with a net negative charge and lack of amino acids such as tryptophan, histidine, proline, and phenylalanine are a hallmark of the CDRs in BOV LC and the bovine V30 germline.

Remarkably, grafting the CDRs from BOV LC can improve the secretion, stability, and homogeneity of human LCs. Although the grafting of bovine CDRs on LCs of human therapeutic antibodies may raise immunogenicity concerns, new machine learning tools could be used to test which sequences exhibit the highest degree of humanness (Ramon et al., 2024). This finding opens an exciting opportunity to use sequence features from the V30 germline to improve the biophysical properties of diagnostic and therapeutic antibodies.

Thus, the analysis of the highly conserved cow antibody domains revealed biophysical features intrinsic to LCs that are not subjected to selection pressure for antigen binding, which can inform the design of antibodies with improved properties.

4 | MATERIALS AND METHODS

4.1 | Protein production

LC sequences were ordered from commercial gene synthesis (GeneArt, Thermo Fisher) and cloned into a pcDNA3.1(+) vector. XL-1 *E. coli* cells were transformed

with the plasmids and colonies were selected on ampicillin LB-agar plates. Plasmids were purified from overnight cultures of transformed XL-1 cells using a PureYield™ kit (Promega). The correct inserts were verified by Sanger sequencing. LCs were produced using the Expi293 or ExpiCHO systems (Thermo Fisher) following manufacturers' protocols with ExpiFectamine (Thermo Fisher) or jetOPTIMUS (Polyplus). For head-to-head comparisons of LC secretion, Expi293 cells and reagents were used. Secreted LCs were first purified by anion exchange chromatography or cation exchange chromatography using a HiTrap™ Q HP (cytiva) or a HiTrap™ SP FF (cytiva) column. Subsequently, LCs were also purified with hydrophobic interaction chromatography on a HiTrap™ Butyl column (cytiva). The final purification step was size-exclusion chromatography with a HiLoad® 16/60 Superdex® 75 pg column (cytiva). All analytical measurements were performed in phosphate-buffered saline (PBS) unless otherwise stated.

4.2 | SDS-PAGE

Samples were mixed with Lämmli and heated for 5 min at 95 °C. For reducing conditions, 10 mM dithiothreitol was added before heat denaturation. Dual Color Protein Standard III (Serva) was used as a molecular weight ladder. The denatured samples and the ladder were resolved on 4%–20% gradient gels (Serva) following manufacturer's recommendations. The gels were stained with a Quick Coomassie stain (Serva) and destained in ultrapure water following the manufacturer's protocol.

4.3 | SEC-MALS

A Shimadzu HPLC with a UV and a refractive index detector coupled to a Heleos II MALS detector (Wyatt Technology) were used. The LCs were injected on a Superdex™ 200 Increase 10/300 GL column (cytiva) with PBS as running buffer using a constant mobile phase flow of 0.5 mL/min unless otherwise stated. Data collection and analysis was performed with the ASTRA v5. Each sample was measured at least in duplicates.

4.4 | FUV-CD

Measurements were performed on a J-1500 CD spectrometer (Jasco) using a 1 mm quartz cuvette and a protein concentration of 0.1 mg/mL. CD spectra were collected at 20 °C. For the thermal melts, the CD signal at 202 nm was measured while the sample was heated from 20 to 90 °C in 0.5 °C steps.

AUTHOR CONTRIBUTIONS

Hristo L. Svilenov: Writing – original draft; conceptualization; funding acquisition; writing – review and editing; supervision; resources. **Johanna Trommer:** Writing – review and editing; methodology; formal analysis; investigation. **Florian Lesniowski:** Writing – review and editing; methodology; formal analysis. **Johannes Buchner:** Writing – review and editing; conceptualization; funding acquisition; resources; supervision.

ACKNOWLEDGMENTS

This work was supported by grants from the Peter und Traudl Engelhorn Stiftung (postdoctoral fellowship) and funding from the Else Kröner-Fresenius-Stiftung (2020_EKEA.31) to H.L.S. Open Access funding enabled and organized by Projekt DEAL.

ORCID

Johannes Buchner https://orcid.org/0000-0003-1282-7737

Hristo L. Svilenov https://orcid.org/0000-0001-5863-9569

REFERENCES

Adams R, Joyce C, Kuravskiy M, Harrison K, Ahdash Z, Balmforth M, et al. Serum albumin binding knob domains engineered within a VH framework III bispecific antibody format and as chimeric peptides. Front Immunol. 2023;14:1170357.

Chi X, Li Y, Qiu X. V(D)J recombination, somatic hypermutation and class switch recombination of immunoglobulins: mechanism and regulation. Immunology. 2020;160:233–47.

de los Rios M, Criscitiello MF, Smider VV. Structural and genetic diversity in antibody repertoires from diverse species. Curr Opin Struct Biol. 2015;33:27–41.

Deiss TC, Vadnais M, Wang F, Chen PL, Torkamani A, Mwangi W, et al. Immunogenetic factors driving formation of ultralong VH CDR3 in *Bos taurus* antibodies. Cell Mol Immunol. 2019;16:64–75.

Dong J, Finn JA, Larsen PA, Smith TPL, Crowe JE. Structural diversity of ultralong CDRH3s in seven bovine antibody heavy chains. Front Immunol. 2019;10:558.

Feige MJ, Groscurth S, Marcinowski M, Shimizu Y, Kessler H, Hendershot LM, et al. An unfolded CH1 domain controls the assembly and secretion of IgG antibodies. Mol Cell. 2009;34:569–79.

Garces F, Lee JH, de Val N, Torrents de la Pena A, Kong L, Puchades C, et al. Affinity maturation of a potent family of HIV antibodies is primarily focused on accommodating or avoiding glycans. Immunity. 2015;43:1053–63.

Greenberg AS, Avila D, Hughes M, Hughes A, McKinney EC, Flajnik MF. A new antigen receptor gene family that undergoes

rearrangement and extensive somatic diversification in sharks. Nature. 1995;374:168–73.
Hamers-Casterman C, Atarhouch T, Muyldermans S, Robinson G, Hammers C, Songa EB, et al. Naturally occurring antibodies devoid of light chains. Nature. 1993;363:446–8.
Hawkins A, Joyce C, Brady K, Hold A, Smith A, Knight M, et al. The proximity of the N- and C- termini of bovine knob domains enable engineering of target specificity into polypeptide chains. MAbs. 2022;14:2076295.
Jayaram N, Bhowmick P, Martin ACR. Germline VH/VL pairing in antibodies. Protein Eng Des Sel. 2012;25:523–30.
Jespers L, Schon O, Famm K, Winter G. Aggregation-resistant domain antibodies selected on phage by heat denaturation. Nat Biotechnol. 2004;22:1161–5.
Lee JH, Andrabi R, Su CY, Yasmeen A, Julien JP, Kong L, et al. A broadly neutralizing antibody targets the dynamic HIV envelope trimer apex via a long, rigidified, and anionic β-hairpin structure. Immunity. 2017;46:690–702.
Li TT, Xia T, Wu JQ, Hong H, Sun ZL, Wang M, et al. De novo genome assembly depicts the immune genomic characteristics of cattle. Nat Commun. 2023;14:6601.
Liljavirta J, Niku M, Pessa-Morikawa T, Ekman A, Iivanainen A. Expansion of the preimmune antibody repertoire by junctional diversity in *Bos taurus*. PloS One. 2014;9:e99808.
Ma L, Qin T, Chu D, Cheng X, Wang J, Wang X, et al. Internal duplications of DH, JH, and C region genes create an unusual IgH gene locus in cattle. J Immunol. 2016;196:4358–66.
Macpherson A, Laabei M, Ahdash Z, Graewert MA, Birtley JR, Schulze MSED, et al. The allosteric modulation of complement c5 by knob domain peptides. elife. 2021;10:1–49.
Macpherson A, Scott-Tucker A, Spiliotopoulos A, Simpson C, Staniforth J, Hold A, et al. Isolation of antigen-specific, disulphide-rich knob domain peptides from bovine antibodies. PLoS Biol. 2020;18:e3000821.
Passon M, De Smedt SC, Svilenov HL. Principles of antibodies with ultralong complementarity-determining regions and picobodies. Biotechnol Adv. 2023;64:108120.
Rabia LA, Desai AA, Jhajj HS, Tessier PM. Understanding and overcoming trade-offs between antibody affinity, specificity, stability and solubility. Biochem Eng J. 2018;137:365–74.
Ramon A, Ali M, Atkinson M, Saturnino A, Didi K, Visentin C, et al. Assessing antibody and nanobody nativeness for hit selection and humanization with AbNatiV. Nat Mach Intell. 2024;6:74–91.
Ren J, Nettleship JE, Harris G, Mwangi W, Rhaman N, Grant C, et al. The role of the light chain in the structure and binding activity of two cattle antibodies that neutralize bovine respiratory syncytial virus. Mol Immunol. 2019;112:123–30.
Saini SS, Farrugia W, Ramsland PA, Kaushik AK. Bovine IgM antibodies with exceptionally long complementarity-determining region 3 of the heavy chain share unique structural properties conferring restricted $V_H + V_\lambda$ pairings. Int Immunol. 2003;15:845–53.
Sok D, le KM, Vadnais M, Saye-Francisco KL, Jardine JG, Torres JL, et al. Rapid elicitation of broadly neutralizing antibodies to HIV by immunization in cows. Nature. 2017;548:108–11.
Stanfield RL, Berndsen ZT, Huang R, Sok D, Warner G, Torres JL, et al. Structural basis of broad HIV neutralization by a vaccine-induced cow antibody. Sci Adv. 2020;6:eaba0468.
Stanfield RL, Haakenson J, Deiss TC, Criscitiello MF, Wilson IA, Smider VV. The unusual genetics and biochemistry of bovine immunoglobulins. Adv Immunol. 2018;137:135–64.
Stanfield RL, Wilson IA, Smider VV. Conservation and diversity in the ultralong third heavy-chain complementarity-determining region of bovine antibodies. Sci Immunol. 2016;1:aaf7962.
Svilenov HL, Sacherl J, Protzer U, Zacharias M, Buchner J. Mechanistic principles of an ultra-long bovine CDR reveal strategies for antibody design. Nat Commun. 2021;12:6737.
Wang F, Ekiert DC, Ahmad I, Yu W, Zhang Y, Bazirgan O, et al. Reshaping antibody diversity. Cell. 2013;153:1379–93.

SUPPORTING INFORMATION

Additional supporting information can be found online in the Supporting Information section at the end of this article.

How to cite this article: Trommer J, Lesniowski F, Buchner J, Svilenov HL. Specific features of a scaffolding antibody light chain. Protein Science. 2024;33(5):e4990. https://doi.org/10.1002/pro.4990